ELSEVIER

Materials Science and Engineering B 147 (2008) 276–279

MATERIALS SCIENCE & ENGINEERING B

www.elsevier.com/locate/mseb

Thermally evaporated In_2O_3 nanoloquats with oxygen flow-dependent optical emissions

Chia-Pu Chu [1], Tsung-Shine Ko [1], Yu-Cheng Chang [1], Tien-Chang Lu *, Hao-Chung Kuo *, Shing-Chung Wang [1]

Department of Photonics & Institute of Electro-Optical Engineering, National Chiao Tung University, 1001 Ta Hsueh Road, Hsinchu 30050, Taiwan, ROC

Received 28 June 2007; received in revised form 9 August 2007; accepted 28 August 2007

Abstract

We report the synthesis of the In_2O_3 nanoloquat grown at different oxygen flow rates by using the thermal evaporation method. The gold nanoparticles were used as the catalyst and were dispersed on the silicon wafer to facilitate the growth of In_2O_3 nanoloquats. The nanostructures of the In_2O_3 nanoloquats were characterized by scanning electron microscopy, transmission electron microscopy and X-ray diffraction. The photoluminescence (PL) study reveals that In_2O_3 nanoloquats could emit different luminescence peaks in the range of 500–600 nm with broad bands by adjusting different oxygen flow rates. The coverage of the wavelength tuning in the emission peaks of the In_2O_3 nanoloquats could be beneficial for possible applications in white light illumination through manipulating the ratio of each wavelength component.

Keywords: Nanostructure; In_2O_3; Photoluminescence; White light emission

1. Introduction

In_2O_3 is an important transparent semiconductor material with wide bandgap energy (3.6 eV), which has been applied in optical and electric devices such as solar cells and liquid crystal devices [1–3]. Previous studies focused on the preparations and characterizations of In_2O_3 films or nanostructrues [4,5], however, the photoluminescence (PL) results of In_2O_3 varied a lot obtained by different research groups in terms of optical properties. For instance, Lee et al. obtained the PL emission of 637 nm from the In_2O_3 thin films synthesized by thermal oxidation [4]. Liang et al. used InP as the starting material to grow In_2O_3 nanofibers using a furnace and their PL spectra exhibited emission of 470 nm [6]. Zheng et al. observed the PL emission of 429 and 460 nm from their In_2O_3 nanowires using a three-probe dc method [7]. Li et al. measured PL of the In_2O_3 nanotubes exhibiting emission of 593 nm [8]. Most of the above PL results come from different densities of oxygen vacancies [9,10]. However, few groups have developed methods to modulate the emissive wavelength of In_2O_3. Therefore, what inspires us to delve into the origin and the modulation of the emissive wavelength originates from that accordingly. In this paper, we report the synthesis of In_2O_3 nanoparticles with a special shape similar to the loquat using the two-zone thermal evaporation method. The PL results exhibited different broad band emission peaks ranging from 500 nm to 600 nm when In_2O_3 nanoloquats were grown by adjusting oxygen flow rates, which could have potential applications to white light illumination.

2. Experiment technologies

2.1. Synthesis of In_2O_3 nanoloquats

The synthesis procedures of In_2O_3 nanoloquats started with gold nanoparticles produced by the chemical reduction of gold chloride tetrahydrate ($HAuCl_4$) with sodium citrate spread onto the Si substrates cleaned by the 3-aminopropyl-trimethoxysilan (APTMS) ethanol solution and water. Observed from the SEM images, the Au nanoparticles are 10–20 nm in width and the density is around 6×10^8 cm^{-2}. Then, the gold nanoparticles on Si substrates were then sent to a two-zone vacuum furnace to grow

* Corresponding authors. Tel.: +886 3 5712121x52962; fax: +886 3 5716631.
E-mail addresses: timtclu@faculty.nctu.edu.tw (T.-C. Lu), hckuo@faculty.nctu.edu.tw (H.-C. Kuo).
[1] Tel.: +886 3 5712121x52962; fax: +886 3 5716631.

0921-5107/$ – see front matter © 2007 Published by Elsevier B.V.
doi:10.1016/j.mseb.2007.08.024

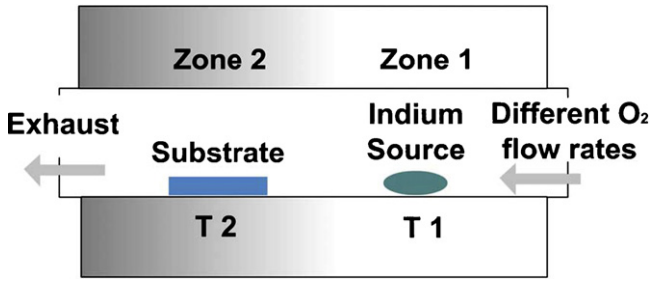

Fig. 1. Schematic diagram of a two-zone furnace for indium oxide nanoloquats growth.

the In_2O_3. The experimental setup for synthesizing indium oxide nanoloquats is schematically depicted in Fig. 1. The starting material, 5 g indium metal, was placed in a quartz boat located inside a quartz tube reactor, designated as zone 1 with the temperature setting as *T*1. p-type silicon (1 0 0) substrates were placed in the downstream of the tube reactor separated from the starting material by 20 cm, designated as zone 2 with the temperature setting as *T*2. The quartz tube was exhausted by a mechanical pump down to around 0.1 Torr. We grew indium oxide nanoloquats under different oxygen flow rates from 50 to 200 sccm for 8 h reaction time. The temperature *T*1 was set 900 °C for the source zone and the temperature *T*2 was set 700 °C for the reaction zone.

2.2. Apparatus

Speaking of characterization, scanning electron microscopy (SEM, by JEOL, JSM 6500F) and high-resolution transmission electron microscopy (HRTEM, by JEOL, JEM 2010F, operating at 200 kV) were used for investigation of the morphology and microstructure of the as-grown samples. The compositions were analyzed using energy dispersive spectrometry (EDS) attached to the SEM. Selected area electronic diffraction (SAED) confirmed the crystal orientation of In_2O_3 nanocrystals. The crystal structure analysis was performed by the XRD measurement with Cu Kα radiation. PL spectra were measured at room temperature

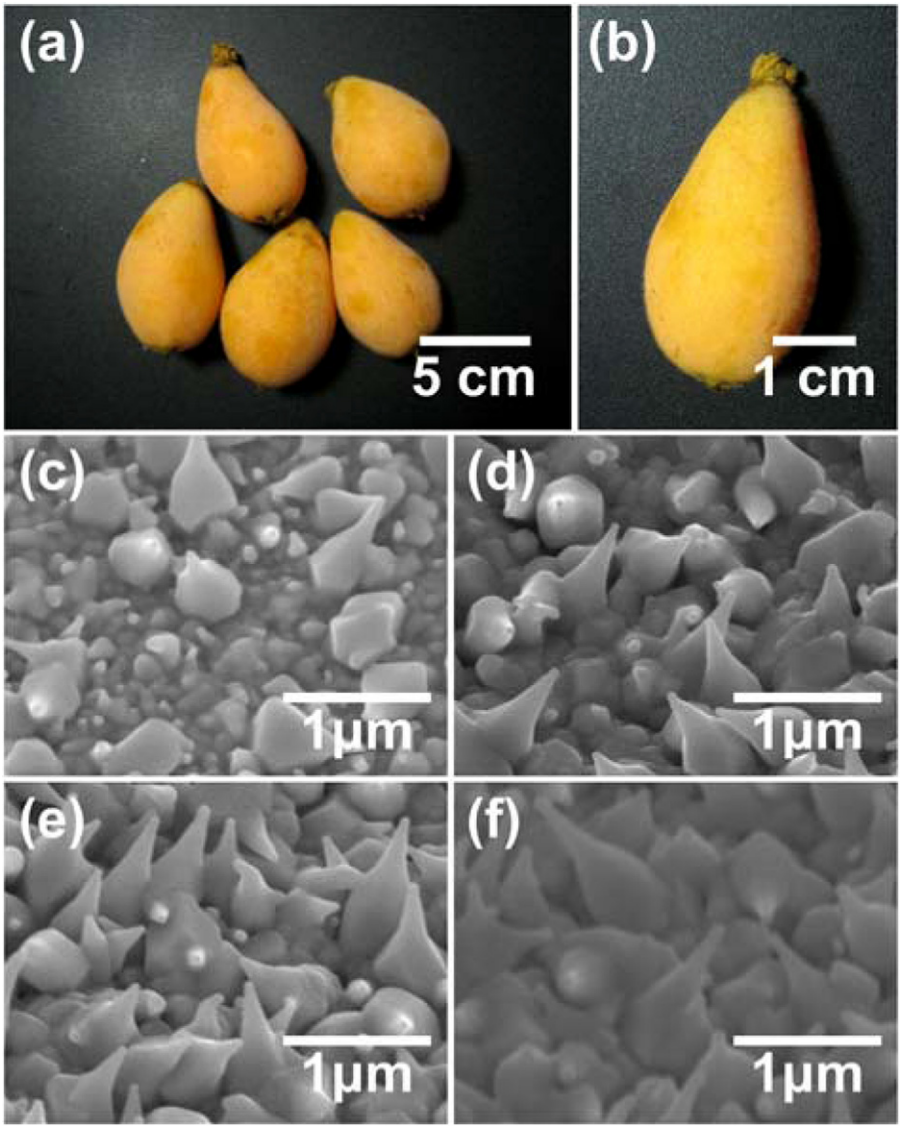

Fig. 2. (a, b) Real loquats shot in Taiwan. (c)–(f) In_2O_3 nanoloquats grown by using different oxygen flow rates of 50, 100, 150 and 200 sccm, respectively.

with a spectrometer (TRIAX-320) excited by a 25 mW He–Cd laser with the emission wavelength of 325 nm.

3. Results and discussion

3.1. Structure analysis of In_2O_3 nanoloquats

Fig. 2(c)–(f) shows SEM images of the In_2O_3 nanocrystals grown at different oxygen flow rates in the range 50, 100, 150 and 200 sccm, respectively, by using the thermal oxidation method with the growth temperature of 700 °C. The name of In_2O_3 nanoloquat derives from special shapes of these nanocrystals similar to the real loquat fruits as shown in Fig. 2(a) and (b) [11]. The amount of nanoloquat was found to be dependent on the oxygen flow rate. As a result, Fig. 2(c) shows fewer nanoloquats existed and many In_2O_3 tips are beginning to sprout when the oxygen flow rate was 50 sccm. As the oxygen flow rate was increased to 200 sccm, most of In_2O_3 nanocrystals show well-shaped loquat as indicated in Fig. 2(f).

The HRTEM images of the nanoloquat grown with the oxygen flow rate of 150 sccm at 700 °C are shown in Fig. 3(a) and (b). It is clearly shown that the In_2O_3 nanoloquat was capped with a 20 nm gold nanoparticle. The presence of gold nanoparticles at the top of the In_2O_3 nanoloquats provides a strong evidence for a vapor–liquid–solid (VLS) growth mechanism. However, VLS growth mechanism generally leads to a well directional growth and further to form nanowire or nanorod structures [12,13], which is different from our results. We proposed that the short In_2O_3 nanowires were nucleated at the gold nanoparticles by the VLS mechanism at first. As the growth time passed by, the growth direction still favored to the top due to the fast reaction provided by the catalyst. However, the over-supply of the indium vapor interacting with oxygen atoms could further facilitate the lateral growth, the lateral volume could increase and then turned into the loquat shape. Fig. 3(c) and (d) shows HRTEM image of a partial In_2O_3 nanoloquat and the corresponding SAED result, which proved our In_2O_3 nanoloquat was a single crystal structure. The lattice plane of (4 2 2) with an interplanar spacing of 0.207 nm and (6 2 2) with spacing of 0.153 nm can be obtained by the analysis of both TEM images and SAED shown in Fig. 3 corresponding to the In_2O_3 crystal lattice planes.

Typical XRD patterns of the In_2O_3 nanoloquats grown with different oxygen flow rates are shown in Fig. 4. All the diffraction peaks could be indexed to a pure cubic phase structure with a lattice constant of $a = 1.011$ Å (JCPDS 71-2195). Both measurement results show that the stronger and sharper XRD phase peaks could be detected as the oxygen flow rates were increased. Therefore, the crystalline quality of In_2O_3 nanoloquats could be improved by means of adjusting oxygen flows, which was consistent with our SEM observations.

3.2. Optical properties of In_2O_3 nanoloquats

The normalized PL measurement results of the In_2O_3 nanoloquats prepared by different growth conditions reveal the quality-dependent characteristics as shown in Fig. 5. Since the

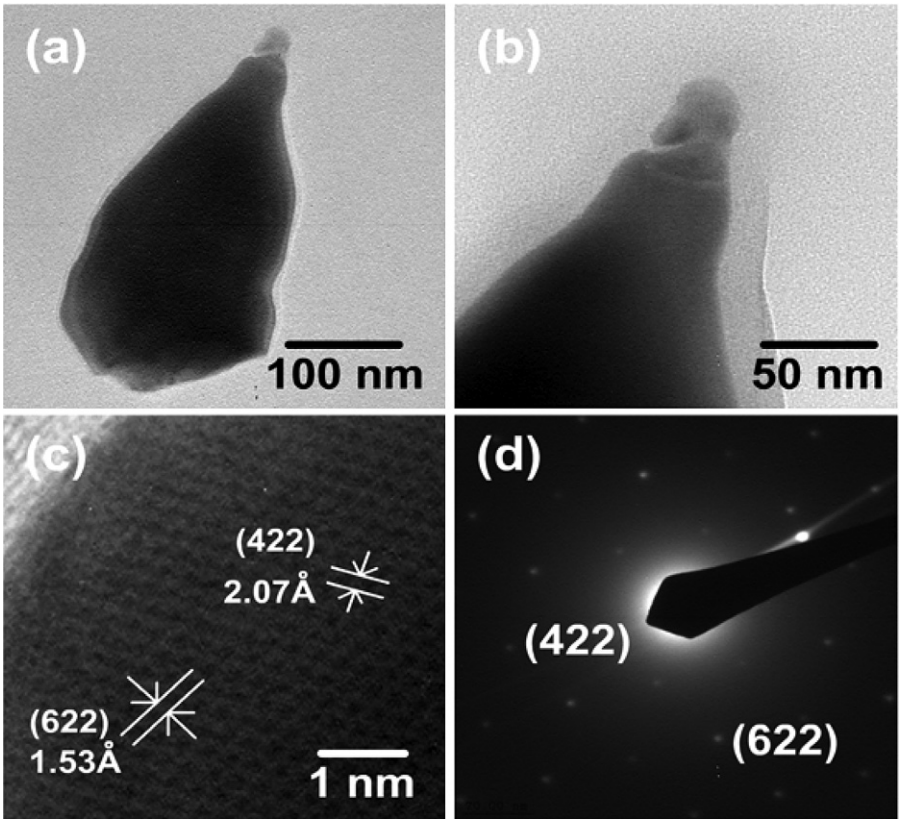

Fig. 3. (a, b) TEM images of the In_2O_3 a nanoloquat's tip. (c) High-resolution TEM images of part of the In_2O_3 nanoloquats. (d) The corresponding selected area electron diffraction pattern.

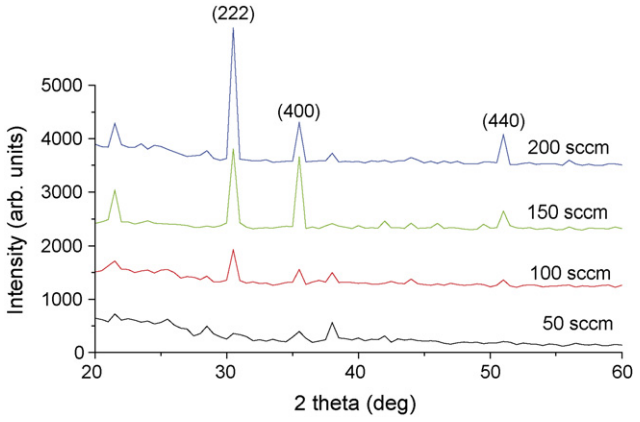

Fig. 4. XRD pattern of the In_2O_3 nanoloquats grown at different oxygen flow rates.

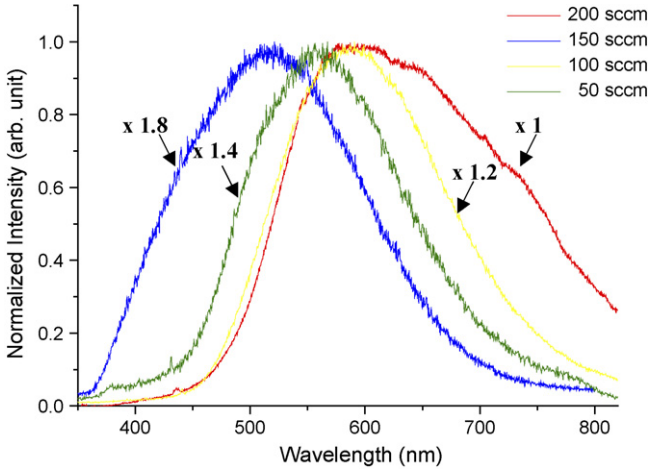

Fig. 5. Room temperature PL spectra of the In_2O_3 nanoloquats grown at different oxygen flow rates.

bandgap energy of In_2O_3 is around 3.6 eV, we could boldly obviate the origin of the photoluminescence as shown in Fig. 5 from the band-to-band transition. Namely, the transition could substantially be ascribed to the carrier recombination between the valence band and the oxygen vacancies induced donor levels formed in the midst of the In_2O_3 bandgap [14]. However, the different crystallization quality of the In_2O_3 nanoloquats could result in different transition path of carriers due to the different amounts of oxygen vacancies and defects generated during the growth [5,15]. Therefore, in our case, the worse quality would lead to a shorter wavelength emission due to more oxygen vacancies formed in the nanoloquats grown in conditions of different oxygen flow rates. By adjusting these growth conditions, we could synthesize the In_2O_3 nanoloquats emitting different wavelength emission to span the whole blue-orange light region. It is worth noting that how the oxygen flow rates influenced the optical transition route. Considering the oxygen vacancies, once we increased the oxygen flow rate the vacancies could be repaired and got diminished in amount accordingly. In the theoretical view, fewer oxygen vacancies lead to fewer electrons exists in the indium oxide compound semiconductor. As a result, the Fermi-level descends to the lower energy side. Then the electrons will reside in the lower oxygen vacancies induced donor levels, accompanying the Fermi-level lowering to obtain the narrower optical transition width. Simply put, the more oxygen infusion, the longer wavelength emission could be anticipated.

4. Conclusion

In conclusion, we have grown the In_2O_3 nanoloquat under different oxygen flow rates and using the thermal evaporation method. The VLS process was dominant in the growth of the In_2O_3 nanoloquats confirmed by the TEM images. The single crystal structures of the In_2O_3 nanoloquats were also characterized by the SEM, TEM and X-ray diffraction. The PL measurement results showed that In_2O_3 nanoloquats could emit different broadband luminescence peaks ranging from 500 to 600 nm by adjusting oxygen flow rates. Owing to the different amount of oxygen vacancies provided by different growth conditions, the optical transition energy of the In_2O_3 nanoloquats becomes tunable, which could be beneficial for possible applications in white light illumination.

Acknowledgements

This work was supported by the MOE ATU program and in part by the National Science Council NSC 95-2120-M-009-008, NSC 95-2752-E-009-007-PAE and NSC 95-2221-E-009-282, Republic of China.

References

[1] M. Emziane, R.L. Ny, Mater. Res. Bull. 35 (2000) 1849.
[2] I. Hamberg, C.G. Granqvist, J. Appl. Phys. 60 (1986) R123.
[3] C.G. Granqvist, Appl. Phys. A: Mater. Sci. Process 57 (1993) 19.
[4] M.S. Lee, W.C. Choi, E.K. Kim, C.K. Kim, S.K. Min, Thin Solid Films 279 (1996) 1.
[5] D.A. Magdas, A. Cremades, J. Piqueras, Appl. Phys. Lett. 88 (2006) 113107.
[6] C. Liang, G. Meng, Y. Lei, F. Phillipp, L. Zhang, Adv. Mater. 13 (2001) 1330.
[7] M.J. Zheng, L.D. Zhang, G.H. Li, X.Y. Zhang, X.F. Wang, Appl. Phys. Lett. 79 (2001) 839.
[8] Y. Li, Y. Bando, D. Golberg, Adv. Mater. 15 (2003) 581.
[9] C.H. Liang, G.W. Meng, Y. Lei, F. Phillip, L.D. Zhang, Adv. Mater. 13 (2001) 1330.
[10] D.A. Magdas, A. Cremades, J. Piqueras, Appl. Phys. Lett. 88 (2006) 113107–113111.
[11] http://en.wikipedia.org/wiki/Loquat.
[12] C.H. Liang, L.C. Chen, J.S. Hwang, K.H. Chen, Y.T. Hung, Y.F. Chen, Appl. Phys. Lett. 81 (2002) 22.
[13] H.J. Chun, Y.S. Choi, S.Y. Bae, H.C. Choi, J. Park, Appl. Phys. Lett. 85 (2004) 461.
[14] H. Cao, X. Qiu, Y. Liang, Q. Zhu, M. Zhao, Appl. Phys. Lett. 83 (2003) 761.
[15] K.B. Sundaram, G.K. Bhagavat, Phys. Status Solidi 63 (1987) K15.